BIOCHEMISTRY
including biophysical chemistry & molecular biology

Article

pubs.acs.org/biochemistry

In Calmodulin–IQ Domain Complexes, the Ca^{2+}-Free and Ca^{2+}-Bound Forms of the Calmodulin C-Lobe Direct the N-Lobe to Different Binding Sites

D. J. Black and Anthony Persechini*

Division of Molecular Biology and Biochemistry, University of Missouri, Kansas City, Missouri 64110-2499, United States

ABSTRACT: We have investigated the roles played by the calmodulin (CaM) N- and C-lobes in establishing the conformations of CaM–IQ domain complexes in different Ca^{2+}-free and Ca^{2+}-bound states. Our results indicate a dominant role for the C-lobe in these complexes. When the C-lobe is Ca^{2+}-free, it directs the N-lobe to a binding site within the IQ domain consensus sequence. It appears that the N-lobe must be Ca^{2+}-free to interact productively with this site. When the C-lobe is Ca^{2+}-bound, it directs the N-lobe to a site upstream of the consensus sequence, and it appears that the N-lobe must be Ca^{2+}-bound to interact productively with this site. A model for switching in CaM–IQ domain complexes is presented in which the N-lobe adopts bound and extended positions that depend on the status of the Ca^{2+}-binding sites in each CaM lobe and the compositions of the two N-lobe binding sites. Ca^{2+}-dependent changes in the conformation of the bound C-lobe that appear to be responsible for directed N-lobe binding are also identified. Changes in the equilibria between extended and bound N-lobe positions may control bridging interactions in which the extended N-lobe is bound to another CaM-binding domain. Ca^{2+}-dependent control of bridging interactions with CaM has been implicated in the regulation of ion channel and unconventional myosin activities.

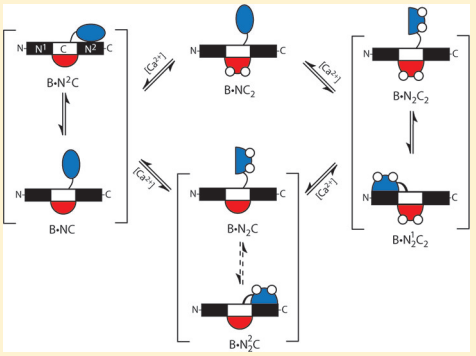

Through an interactome of at least 100 proteins playing roles in essentially all biological functions, the Ca^{2+}-binding protein calmodulin (CaM) helps to orchestrate the cellular response to a Ca^{2+} signal. CaM is comprised of globular N- and C-lobes connected by a flexible tether sequence.[1−3] Each lobe contains a pair of EF hand Ca^{2+}-binding sites.[4] Because of cooperativity within each pair of sites, $(Ca^{2+})_2$-CaM, with Ca^{2+} bound to the N- or C-lobe, and $(Ca^{2+})_4$-CaM, with Ca^{2+} bound to both lobes, are the major Ca^{2+}-bound species produced.[5] Although there is no broad consensus CaM-binding sequence in proteins, a large class that includes unconventional myosins, several ion channels, and modulators of small GTPases bind CaM through IQ domains, which are commonly identified on the basis of the consensus sequence, [I,L,V]-Q*xxx*R[G,*x*]*xxx*[R,K].[6−9] Many CaM–IQ domain complexes are maintained in the presence and absence of Ca^{2+}, a property we have exploited to investigate the transitions between Ca^{2+}-free and Ca^{2+}-bound forms of these complexes.[10−12]

Structural data suggest that Ca^{2+}-free CaM makes at least two types of complexes with IQ domains. One is compact, with both N- and C-lobes bound to the IQ domain consensus region.[13,14] In the other, the N-lobe adopts a mobile, extended position.[14−16] The bound N-lobe conformation appears to require a semiconserved G residue within the N-lobe binding site.[13,14] In both types of Ca^{2+}-free complexes, the IQ domain is in a helical conformation, and the CaM C-lobe is bound in a parallel orientation (with respect to amino acid sequence) to a site that includes the consensus "IQ".[13,15,16] In structures that have been determined for Ca^{2+}-saturated CaM–IQ domain complexes, the C-lobe also is bound in a parallel orientation to this site, but the N-lobe is bound to a site upstream of the IQ domain consensus region.[17,18] Because Ca^{2+}-free and Ca^{2+}-bound structures have not been determined for a single CaM–IQ domain complex, it is unclear whether the N-lobe is able to move from one binding site to another in response to changes in the free Ca^{2+} concentration.

We recently have investigated how Ca^{2+}-dependent switching in a reference CaM–IQ domain complex is affected by various amino acid replacements in the IQ domain.[10,19] Our results suggested a model in which the Ca^{2+}-free C-lobe and the Ca^{2+}-bound C-lobe direct the N-lobe to different binding sites in an IQ domain.[10,19] In this paper, we confirm and extend this model on the basis of an analysis of the affinity contributions of the CaM N-lobe in the reference complex and variants with amino acid replacements in the two putative N-lobe binding sites.

MATERIALS AND METHODS

CaM binding data were generated using fluorescent protein reporters containing IQ domain insert sequences derived from neuromodulin. Similar reporters have been described in detail previously.[12,20,21] The extent of fluorescence resonance energy transfer (FRET) from a cyan fluorescent protein donor (ECFP) to a yellow acceptor (EYFP) is decreased when

Received: August 15, 2011
Revised: October 4, 2011
Published: October 14, 2011

CaM is bound to the insert.[12,20,21] The inserts in two of the reporters used here, B_{IQ} and EB_{IQ}, are listed in Figure 1. Those

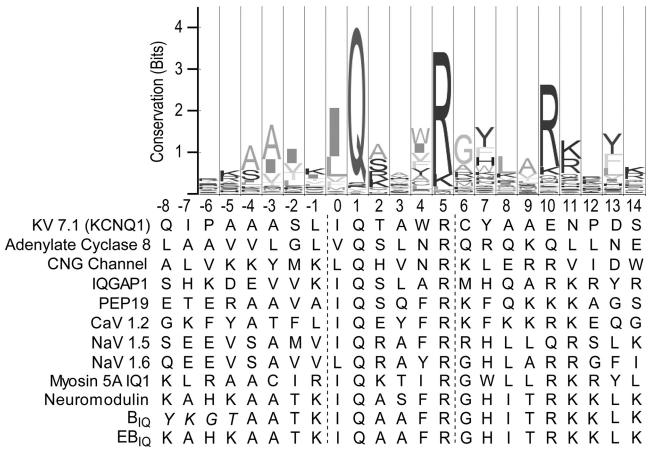

Figure 1. IQ domains are found in proteins with diverse functions. A logo representation of a hidden Markov model profile derived from ~3000 IQ domain sequences in the Pfam-A database is presented.[47,48] Each position is represented by a stack of one-letter amino acid symbols. The total height of a stack is an indication of how well-conserved that position is, and the height of each amino acid symbol in a stack is an indication of its relative frequency. The individual amino acid sequences listed below this profile correspond with the IQ domains in several representative proteins and the insert sequences in the B_{IQ} and EB_{IQ} reporters. Sequences are numbered in relation to the I residue in the common IQ domain consensus sequence, [I,L,V]-Q*xxx*R[G,*x*]*xxx*[R,K], which was used to identify the profiled sequences. The region in italics in the B_{IQ} sequence is a fluorescent protein sequence, which is replaced in EB_{IQ} by the neuromodulin sequence, KAHK. The structures presented in Figure 3A are for CaM bound to the myosin 5A, NaV 1.5, and CaV 1.2 domains listed here.

in the other reporters contain amino acid replacements in the IQ domain as specified in the text and captions. Two mutant CaMs were employed to delineate the effects of Ca^{2+} binding to each CaM lobe: N_xCCaM (N_xC), in which Ca^{2+} ligands at positions 31 and 67 in the N-lobe EF hand pair have been replaced with Ala, and NC_xCaM (NC_x), in which the homologous ligands at positions 104 and 140 in the C-lobe EF hands have been replaced.[12] We have previously established the mutant EF hand pairs do not bind Ca^{2+} under our experimental conditions.[12] In the absence of Ca^{2+}, both mutant CaMs bind IQ domains with affinities and rate constants essentially identical to those determined for native CaM.[11,12] Native and mutant CaMs and the C-lobe fragment (CaM residues 78−148) were prepared as described previously.[22−25] Fluorescent reporters were prepared using a modified version of the protocol described previously because the EB_{IQ} reporter was found to be susceptible to proteolysis.[22] The following modifications were made. (1) The six-His affinity tag was moved to a C-terminal position, and (2) anion exchange chromatography was performed after Ni^{2+} chelate affinity chromatography. The eluate from the latter was dialyzed against 25 mM Tris-HCl and 0.5 mM DTT (pH 8.0) and applied to a Mono-Q column equilibrated at 4 °C in the same buffer. Reporter proteins were eluted using a 4%/mL linear gradient against 25 mM Tris-HCl, 500 mM NaCl, and 0.5 mM DTT (pH 8.0). Fractions containing the intact reporter were identified on the basis of the ratio of the ECFP and EYFP absorbances at 430 and 515 nm and verified by sodium dodecyl sulfate gel electrophoresis. All of the results presented in this paper were determined using reporters prepared in this manner.

We have previously determined K_d values for CaM complexes with the N-terminally tagged B_{IQ} reporter, and variants with A, R, and M replacements in the IQ domain at position 6.[10] These determinations were repeated using the C-terminally tagged versions of these reporters (Table 1). Moving the six-His tag appears to have had no effect on their CaM binding properties.

Fluorescence Measurements and Analysis of Binding Data. A Photon Technologies International (Monmouth Junction, NJ) QM-1 fluorometer operated in photon counting mode was used for all fluorescence measurements. Monochromator excitation and emission bandwidths were ~2.5 nm. All binding experiments were performed at 23 °C. The standard experimental buffer contained 25 mM Tris (pH 7.5), 100 mM KCl, and 100 μg/mL BSA. Binding isotherms were generated by successive additions of CaM or the C-lobe fragment ligand to a stirred 2 mL quartz cuvette containing 10−100 nM reporter. Nominally Ca^{2+}-free conditions were produced by including 3 mM BAPTA. Saturation of functional Ca^{2+} binding sites in native or mutant CaMs and the C-lobe fragment was in general effected by adding $CaCl_2$ to buffers and CaM stock solutions to produce a final free Ca^{2+} concentration of ~250 μM. Ca^{2+} saturation was verified by adding ~1 mM $CaCl_2$ at the end of each binding experiment. With complexes expected to have very low Ca^{2+} binding affinities because of strongly negative energy coupling, experiments were performed at a free Ca^{2+} concentration of ~3 mM.

Fractional decreases in reporter fluorescence emission at 525 nm (430 nm excitation) are directly proportional to fractional saturation of the IQ domain inserts in these constructs. The fractional reporter response is formally defined as $(F_{max} - F)/(F_{max} - F_{min})$, where F corresponds to the fluorescence emission at 525 nm measured after each addition and F_{max} and F_{min} correspond to the fluorescence of the free and ligand-saturated reporter, respectively. Apparent K_d values were derived using hyperbolic or quadratic binding equations as we have described previously.[12,22] Reported values are the means of estimates derived from three to five independent data sets. Errors are expressed as the standard error of the mean (SEM). The difference between two values is considered statistically significantly if the p value derived using an unpaired t-test is less than 0.05.

RESULTS

Recent structural and biochemical observations suggest that in Ca^{2+}-saturated CaM−IQ domain complexes the CaM N-lobe binds a site upstream of the IQ domain consensus region.[10,17,18] The IQ domain insert in EB_{IQ} therefore contains the upstream neuromodulin sequence, KAHK, that is absent in B_{IQ}, which in effect replaces a fluorescent protein sequence (YKGT) in the latter (Figure 1). Ca^{2+}-saturated CaM binds EB_{IQ} 100 times more tightly than B_{IQ}, consistent with an interaction between the N-lobe and the KAHK sequence (Table 1).

However, this modification also increases the affinity of the Ca^{2+}-free CaM complex (Table 1). This implies an interaction with the C-lobe, because structural data suggest that in Ca^{2+}-free complexes the N-lobe binds a site within the IQ domain consensus region. This effect is largely preserved when the A and H in the KAHK sequence are replaced with E residues, suggesting that it involves one or both of the K residues (Table 1). An examination of several structures determined for

Table 1. K_d Values for Reporter Complexes with CaM and C-Lobe Fragment Species[a]

	K_d (μM)					
reporter	NC	N_2C_x	N_xC_2	N_2C_2	C	C_2
B_{IQ}	2.25 ± 0.10	35.29 ± 1.58	12.07 ± 0.46	2.90 ± 0.11	38.56 ± 2.09	10.56 ± 0.49
EB_{IQ}	0.12 ± 0.02	1.56 ± 0.11	0.39 ± 0.07	0.032 ± 0.004	1.64 ± 0.19	0.39 ± 0.04
$EB_{IQ}A^{-7}E,H^{-6}E$	0.26 ± 0.06	4.35 ± 0.46	2.66 ± 0.44	1.47 ± 0.19	4.86 ± 0.58	2.26 ± 0.18
$B_{IQ}G^6A$	4.76 ± 0.32	898.81 ± 253.37	2.59 ± 0.21	0.79 ± 0.04	11.44 ± 0.75	2.19 ± 0.15
$B_{IQ}G^6R$	5.23 ± 0.39	6.18 ± 0.26	0.89 ± 0.11	0.32 ± 0.01	6.04 ± 0.55	0.95 ± 0.09
$B_{IQ}G^6M$	27.04 ± 1.59	785.45 ± 166.02	2.05 ± 0.18	0.38 ± 0.03	23.01 ± 1.15	1.52 ± 0.19

[a]The insert sequences in B_{IQ} and EB_{IQ} are listed in Figure 1. Representative binding data for the B_{IQ} and EB_{IQ} reporters are presented in Figure 2. The amino acid replacements present in the variant reporters are specified. N and C refer to the N- and C-lobes, respectively, in intact CaM or in the C-lobe fragment (residues 78−148). A subscript *x* indicates a lobe with a disabled EF hand pair, and a subscript 2 indicates that two Ca^{2+} ions are bound to the lobe. The standard experimental buffer contained 25 mM Tris (pH 7.5), 100 mM KCl, and 100 μg/mL BSA. Nominally Ca^{2+}-free conditions were produced by inclusion of 3 mM BAPTA. A free concentration of ~250 μM was employed for most characterizations performed in the presence of Ca^{2+}. Characterizations of the low-affinity N_2C_x complexes with $B_{IQ}G^6A$ and $B_{IQ}G^6M$ were performed at a higher free Ca^{2+} concentration of ~3 mM. At the end of each experiment performed in the presence of Ca^{2+}, saturation of the available Ca^{2+}-binding sites was verified by adding additional aliquots of a $CaCl_2$ solution. Further details are provided in Materials and Methods.

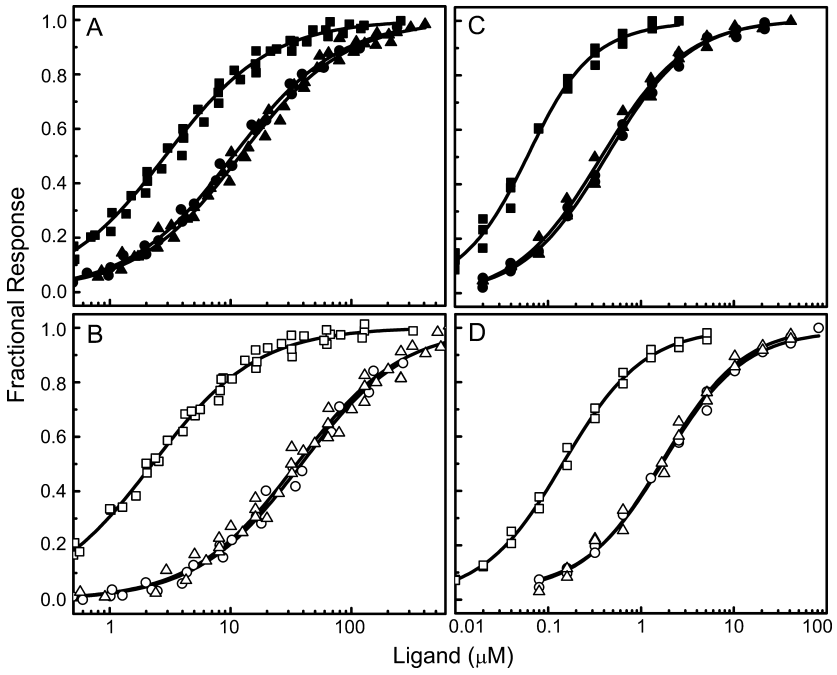

Figure 2. Data for binding of intact CaM and C-lobe fragment to B_{IQ} and EB_{IQ} reporters. Data are presented for B_{IQ} (A and B) and EB_{IQ} (C and D) binding to the following: Ca^{2+}-saturated CaM (■), Ca^{2+}-saturated C-lobe fragment (●), N_xC_2 CaM (▲), Ca^{2+}-free CaM (□), Ca^{2+}-free C-lobe fragment (○), and N_2C_x CaM (△). Apparent K_d values derived from fits (—) of these and similar data to standard binding equations are listed in Table 1. Additional details are provided in Materials and Methods.

CaM−IQ domain complexes indicates that either could interact with the C-lobe.[13,15−18] These observations point to a general difficulty with amino acid substitutions as probes of protein−protein interfaces: They often have multiple effects.

Defining the N-Lobe Affinity Contributions in CaM−IQ Domain Complexes. To confirm and extend our switching model, it was necessary to compare the specific affinity contributions of the N-lobe in reference and variant CaM−IQ domain complexes. These contributions were defined by calculating the ratios of K_d values for reporter complexes with intact CaM and a tryptic fragment (residues 78−148) containing only the C-lobe (Table 2).[25−27] Although in principle a similar analysis could be performed using an N-lobe fragment, this was not attempted because in many instances this lobe appears to make no significant contribution to affinity. The K_d values derived for IQ domain complexes with Ca^{2+}-free and Ca^{2+}-bound forms of intact CaM and the C-lobe fragment are listed in Table 1. These demonstrate that K_d values for the C-lobe fragment are significantly affected by several amino acid replacements in the putative N-lobe binding sites. These effects cancel when the specified K_d ratios are calculated.

Although the CaM lobes appear to behave independently when CaM is free in solution,[5,11,12,28] they must by definition interact when both participate in a peptide or target protein complex.[12,29] Indeed, an interaction between the lobes is clearly demonstrated by the large decreases in affinity seen when Ca^{2+} is bound solely to the N-lobe in the CaM complexes with the $B_{IQ}G^6A$ and $B_{IQ}G^6M$ reporters (Table 1). Apparent N-lobe affinity contributions necessarily include direct and indirect interactions between the lobes. However, this does not prevent us from defining and comparing N-lobe contributions.

Table 2. Ratios of the K_d Values for Reporter Complexes with the C-Lobe Fragment and Intact CaM[a]

	K_d ratio			
reporter	C/NC	C/N_2C_x	C_2/N_xC_2	C_2/N_2C_2
B_{IQ}	17.06 ± 1.21	1.09 ± 0.07	0.88 ± 0.07	3.64 ± 0.22
EB_{IQ}	14.04 ± 2.62	1.06 ± 0.15	0.99 ± 0.21	11.83 ± 1.90
$EB_{IQ}A^{-7}E,H^{-6}E$	18.64 ± 4.66	1.11 ± 0.17	0.85 ± 16	1.54 ± 0.24
$B_{IQ}G^6A$	2.40 ± 0.23	0.013 ± 0.004	0.85 ± 0.09	2.75 ± 0.23
$B_{IQ}G^6R$	1.15 ± 0.14	0.98 ± 0.10	1.06 ± 0.17	2.98 ± 0.31
$B_{IQ}G^6M$	0.85 ± 0.07	0.03 ± 0.01	0.75 ± 0.12	4.03 ± 0.58

[a]These ratios define the affinity contributions of the N-lobe in the complexes with intact CaM. A value of 1 indicates no contribution; a value significantly greater than 1 indicates a positive contribution (increases affinity), and a value significantly less than 1 indicates a negative contribution (decreases affinity).

Analysis of N-Lobe Affinity Contributions. An initial validation of this method of analysis is seen in the K_d ratios for Ca^{2+}-free CaM complexes with B_{IQ} and variants with A, R, and M replacements at position 6 (Table 2). Structural data suggest that a G at this position allows the N-lobe to bind, while the replacements interfere sterically with binding.[13−16,30] Consistent with this, in the CaM complex with B_{IQ}, the N-lobe contributes an ∼17-fold affinity enhancement. This is essentially eliminated by the amino acid replacements which lower the K_d ratio to ∼1. A small N-lobe contribution may remain in the complex with $B_{IQ}G^6A$ (Table 2). The N-lobe contributions in the Ca^{2+}-free CaM complexes with B_{IQ}, EB_{IQ}, and $EB_{IQ}A^{-7}E,H^{-6}E$, which all have a G at position 6, are essentially identical. This is consistent with the idea that the N-lobe binds a site that includes position 6 and does not bind upstream of the IQ domain consensus region (Table 2).

We have previously proposed that when the C-lobe is Ca^{2+}-bound and the N-lobe is Ca^{2+}-free the latter adopts an extended position.[10] Consistent with this, K_d ratios for all the reporter complexes with N_xC_2 CaM are ∼1, suggesting that the N-lobe makes no significant affinity contribution (Table 2). Thus, when Ca^{2+} binds the C-lobe, the Ca^{2+} appears to shift the Ca^{2+}-free N-lobe into an extended position, if it has not already adopted one due to the absence of a G at position 6. We have previously shown that the resulting decrease in the affinity of the complex lowers the Ca^{2+} binding affinity of the C-lobe due to negative energy coupling.[12] In most cases, the CaM C-lobe is expected to bind Ca^{2+} with higher affinity than the N-lobe, so an intermediate Ca^{2+}-bound form with an extended Ca^{2+}-free N-lobe is likely to predominate under equilibrium conditions.[11,12]

The N-lobe contributes an ∼4-fold affinity enhancement in the Ca^{2+}-saturated CaM−B_{IQ} complex, and the A, R, and M replacements at position 6 have little or no effect. This is consistent with binding of the N-lobe to a site upstream of the IQ domain consensus region.[17,18] Extending the neuromodulin sequence into this putative upstream site significantly increases the affinity contribution of the N-lobe, and E substitutions at positions −7 and −6 appear to eliminate any contribution (Table 2). These observations indicate that the N-lobe can adopt extended positions in both Ca^{2+}-saturated and Ca^{2+}-free CaM−IQ domain complexes. This originally was suggested by transient kinetic data demonstrating that a CaM-binding peptide accelerates the dissociation rate for a Ca^{2+}-saturated CaM−IQ domain complex.[11] For this to occur, the peptide must participate in an intermediate bridging complex with one of the CaM lobes.[11]

In some of the complexes with N_2C_x CaM the N-lobe appears to make no significant affinity contribution (Table 1). This suggests that when the C-lobe is Ca^{2+}-free the Ca^{2+}-bound N-lobe adopts an extended position. Given the marked sensitivity of the Ca^{2+}-free N-lobe interaction to replacements at position 6, it is not surprising that this interaction is also disrupted when Ca^{2+} is bound to the N-lobe. An intermediate Ca^{2+}-bound state with an extended Ca^{2+}-bound N-lobe is likely to be important when the free Ca^{2+} concentration is rapidly increased because the N-lobe binds Ca^{2+} much faster than the C-lobe.[11]

The striking negative affinity contributions of the Ca^{2+}-bound N-lobe in the complexes with $B_{IQ}G^6A$ and $B_{IQ}G^6M$ presumably involve interactions between the open hydrophobic cleft in this lobe and the A or M in the IQ domain at position 6 (Table 2). Because of negative energy coupling, millimolar free Ca^{2+} concentrations are required to produce these states, so they are not physiologically relevant. However, their occurrence suggests that the Ca^{2+}-bound N-lobe is unable to interact productively with its putative upstream binding site unless the C-lobe is Ca^{2+}-bound.

DISCUSSION

Structures of Ca^{2+}-free and Ca^{2+}-saturated CaM complexes with different IQ domains suggest that while the C-lobe remains bound in a fixed orientation, the N-lobe can bind a site encompassing position 6 in the IQ domain consensus region, adopt an extended position, or bind a site upstream of the IQ domain consensus region.[13,15−17] Because Ca^{2+}-free and Ca^{2+}-bound structures have not been determined for a single CaM−IQ domain complex, it is unclear whether the N-lobe actually is able to move from one binding site to another, although this is implied.

This paper attempts to address two questions: (1) Can the N-lobe move from one binding site to another in response to changes in the free Ca^{2+} concentration? (2) If so, then what are the roles of the two CaM lobes in this process? Our results suggest that the N-lobe does indeed move from one binding site to another. More importantly, they further suggest that the C-lobe plays a dominant role in this process. When Ca^{2+}-free, the C-lobe directs the N-lobe to a binding site in the IQ domain consensus region; when Ca^{2+}-bound, the C-lobe directs the N-lobe to a site upstream of this region.

A Model for Ca^{2+}-Dependent Switching in CaM Complexes. Results from this laboratory and others are embodied by the model presented in Figure 3B. In this model, the Ca^{2+}-free C-lobe directs the N-lobe to site N^2, which includes position 6 in the IQ domain consensus, while the Ca^{2+}-bound C-lobe directs the N-lobe to site N^1, which is upstream of the IQ domain consensus region. Our results suggest that the equilibria between bound and extended N-lobe positions depend upon the compositions of the N^1 and N^2 sites

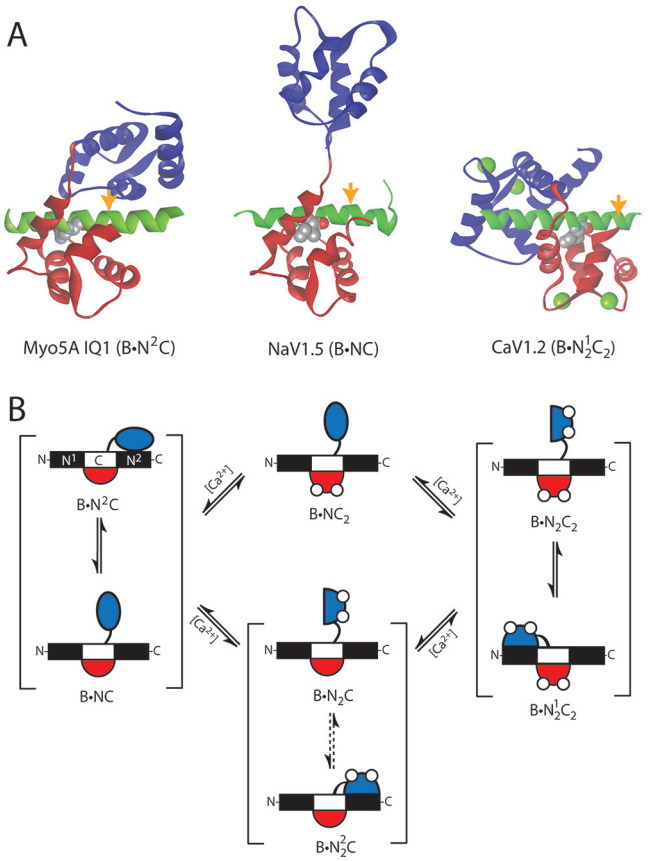

Figure 3. Model for Ca^{2+}-dependent switching in CaM–IQ domain complexes. (A) Structures of CaM bound to IQ domains from myosin 5A, NaV 1.5, and CaV 1.2 (see Figure 1) represent three model states as indicated.[13,15,17] The N- and C-lobes of CaM are colored blue and red, respectively, and bound Ca^{2+} ions are depicted as green spheres. The IQ domain sequences are also colored green. Position 6, which contains a semiconserved G, is denoted with an orange arrow. (B) The N- and C-lobes in CaM are colored blue and red, respectively, and bound Ca^{2+} ions are denoted with empty circles. The N^2 site includes position 6. The N^1 site is upstream of the consensus IQ domain region and in EB_{IQ} includes the KAHK sequence (see Figure 1). The C-lobe is assumed to be bound in a fixed orientation to site C, which includes the consensus IQ amino acid pair. For the sake of clarity, the N^1, C, and N^2 binding sites for the N-lobe are depicted as discrete segments. However, as seen in panel A, the CaM lobes actually interact with overlapping sites on opposing faces of the IQ domain helix. The extended N-lobe is mobile.[15,16]

and whether Ca^{2+} is bound to the N-lobe. The $B{\cdot}N^2{}_2C$ state is unlikely to be produced under physiological conditions, hence the dashed arrows leading to and from it. The C-lobe is assumed to be bound in a fixed orientation to site C, which includes the "IQ" amino acid pair. This is consistent with the structures we have discussed, and the fact that the C-lobe does not appear to dissociate during transitions between its Ca^{2+}-free and Ca^{2+}-bound states.[11] For the sake of clarity, the N^1, C, and N^2 sites are represented as discrete segments, although the CaM lobes actually bind overlapping sites on opposing faces of the IQ domain helix (Figure 3A). The vertical dashed lines in Figure 1 correspond with approximate divisions between the core residues in the three binding sites. Although depicted as fixed, the extended N-lobe is clearly mobile.[15,16]

Because the C-lobe usually binds Ca^{2+} with higher affinity than the N-lobe, under equilibrium conditions the $B{\cdot}NC_2$ state is likely to be the predominant intermediate between Ca^{2+}-free and Ca^{2+}-saturated states.[12] However, under transient conditions, the $B{\cdot}N_2C$ state is likely to become significant because the N-lobe binds Ca^{2+} ions faster than the C-lobe. In fact, transient kinetic data suggest that significant amounts of this state are produced when the free Ca^{2+} concentration is rapidly increased to ≥ 10 μM, which easily can occur in excitable cells.[11,31−36]

How Do the Ca^{2+}-Bound C-Lobe and Ca^{2+}-Free C-Lobe Direct the N-Lobe to the N^1 and N^2 Sites? A structural comparison of the Ca^{2+}-saturated complex between CaM and the IQ domain from the CaV 1.2 channel and the Ca^{2+}-free complex between CaM and IQ domain 1 from myosin 5A is presented in Figure 4. It suggests that the orientation of the first

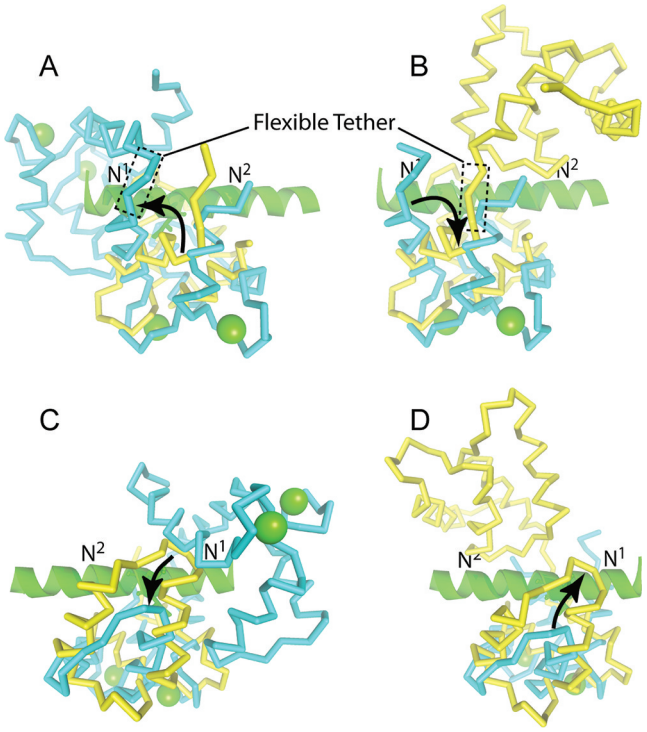

Figure 4. Differences between the Ca^{2+}-bound and Ca^{2+}-free C-lobe that appear to direct the N-lobe to the N^1 and N^2 sites in CaM–IQ domain complexes. The structures shown are for the Ca^{2+}-saturated CaM complex with the IQ domain from the CaV 1.2 channel[17] and the Ca^{2+}-free complex with IQ domain 1 from myosin 5A.[13] The side chains of the consensus I and Q amino acids in the two structures are aligned, which also aligns the IQ domain helices (green). The coordinates for Ca^{2+}-free (yellow) and Ca^{2+}-bound (cyan) CaM are presented as α-carbon tracings. Bound Ca^{2+} ions are depicted as green spheres. The N^1 and N^2 sites in the IQ domains and the flexible tether connecting the two CaM lobes are indicated. The C-lobes (residues 78–148) of both structures are seen in all four panels. In panels A and C, only the Ca^{2+}-bound N-lobe is visible, while in panels B and D, only the Ca^{2+}-free lobe is visible. In panels C and D, the views in panels A and B have been rotated 180° about their vertical axes. Arrows indicate differences in the conformations of the Ca^{2+}-free and Ca^{2+}-bound C-lobes that appear to be determinants of directed N-lobe binding (see the text).

helix in the C-lobe and the position of the loop between the two EF hands in this lobe are determinants of directed N-lobe binding.

To identify these apparent determinants, we aligned the side chains of the consensus I and Q amino acids in the IQ domains in these structures, which also aligns the two IQ domain helices

dx.doi.org/10.1021/bi201300v | Biochemistry 2011, 50, 10061–10068

(green). The coordinates for Ca^{2+}-free (yellow) and Ca^{2+}-bound (cyan) CaM are presented as α-carbon tracings. The Ca^{2+}-free and Ca^{2+}-bound C-lobes (residues 78−148) in the two structures are visible in all four panels. In panels A and C, only the Ca^{2+}-bound N-lobe is visible, while in panels B and D, only the Ca^{2+}-free N-lobe is visible. As indicated by the arrows, in the presence and absence of Ca^{2+}, the orientation of the first helix in the C-lobe changes by ∼45°, which places the attachment point for the flexible tether nearest to the N^1 or N^2 site. This appears to help direct N-lobe binding by controlling its range of motion with respect to the IQ domain. In panels C and D, the views in A and B have been rotated 180° about their vertical axes. The arrows indicate another difference between the Ca^{2+}-bound and Ca^{2+}-free conformations of the C-lobe, which is a change in the position of the loop between the EF hands. When the C-lobe is Ca^{2+}-free, the C-lobe appears to block access to the N^1 site, leaving only the N^2 site available. As noted in Results, the dramatic negative contributions of the Ca^{2+}-bound N-lobes in the complexes between N_2C_x CaM and $B_{IQ}G^6A$ and $B_{IQ}G^6M$ support the idea that the N-lobe cannot access the N^1 site when the C-lobe is Ca^{2+}-free.

What Defines an IQ Domain? The biochemical and structural observations we have discussed suggest that the defining characteristic of the IQ domain family is the presence of site C, which has the consensus sequence [I,L,V]Q*xxx*R. IQ domains in which the N-lobe interacts with neither, one, or both of the N^1 and N^2 sites clearly exist, so domains containing these additional sites appear to represent subfamilies. The basis for conservation of the [I,L,V]Q*xxx*R consensus is evident in the many Ca^{2+}-free structures for CaM or myosin light chain complexes with IQ domains that have been determined.[13,15,16,30] In all of these, the consensus I is inserted into a narrow hydrophobic cleft in the C-lobe, or its light chain homologue, and the consensus Q is coordinated by the loop connecting the two EF hand pairs. The consensus R also interacts with this loop.

As we have noted, a G at position 6 in the N^2 site is a major determinant of whether the N-lobe binds this site with significant affinity (Figure 1). A basic residue at position 10 also appears to participate in this binding interaction.[13,30] The latter position appears better conserved than position 6 (Figure 1). Because N^2 sites lacking a G at position 6 do not appear to bind the N-lobe with significant affinity (Table 2), it is surprising that the two positions are not similarly conserved. Indeed, the IQ domains in adenylate cyclase 8, KV 7.1 K^+, and NaV 1.5 IQ domains are consistent with linkage between these positions as they lack both the G at position 6 and the basic residue at position 10 (Figure 1). Furthermore, the NaV 1.6 IQ domain, which retains the G at position 6, also retains a basic residue at position 10 and so should have a functional N^2 site (Figure 1). This apparent discrepancy may arise from the fact that the IQ domains used to build the HMM profile presented in Figure 1 were identified using the common IQ domain consensus: [I,L,V]Q*xxx*R[G,*x*]*xxx*[R,K], which includes the N^2 site.

The N^1 site appears to be relatively degenerate, compared with the C and N^2 sites. This is not surprising because only the Ca^{2+}-bound N-lobe appears to bind this site (Figure 1). The open, Ca^{2+}-bound conformations of the CaM lobes are notable for the promiscuity of their interactions with amino acid sequences that have little in common besides basic amphipathic character and therefore defy reduction to a consensus pattern.[37,38]

Implications for CaM-Dependent Regulation. The switching model we have proposed includes seven distinct states. In any given CaM−IQ domain complex, the states that predominate depend upon the compositions of the N^1 and N^2 sites. Movements of the N-lobe between bound and extended positions in accordance with this model may control bridging interactions between this lobe and additional CaM-binding sequences. Bridging interactions have been proposed to play roles in the regulation of voltage-gated Ca^{2+} and K^+ channels,[7,39−43] adenylate cyclase 8,[44] and unconventional myosins.[45] These are also necessary intermediates in the transfer of CaM to and from putative CaM storage proteins such as neuromodulin and neurogranin.[11]

The extended Ca^{2+}-bound N-lobe in the $B{\cdot}N_2C$ state, which our results suggest occurs in all CaM−IQ domain complexes when the free Ca^{2+} concentration is increased rapidly, is a likely participant in bridging interactions. Consistent with such a role, in a structure of CaM bound to the gating domain in Ca^{2+}-activated SK channels, the N-lobe forms a bridging interaction in which the Ca^{2+}-bound N-lobe interacts with one domain while the Ca^{2+}-free C-lobe interacts with another.[46] In CaM−IQ domain complexes in which the $B{\cdot}N^1{}_2C_2$ state follows the $B{\cdot}N_2C$ state, bridging interactions with the latter are presumably short-lived. This may be the case in CaV 1.2 channels, whose N^1 sites have sequences that allow the $B{\cdot}N^1{}_2C_2$ state. Bridging interactions initially formed with the $B{\cdot}N_2C$ state are presumably longer-lived in NaV channels because their N^1 sites contain acidic side chains, which should inhibit formation of the $B{\cdot}N^1{}_2C_2$ state (see Figure 1).

AUTHOR INFORMATION

Corresponding Author

*Division of Molecular Biology and Biochemistry, University of Missouri, 5007 Rockhill Rd., Kansas City, MO 64110-2499. Telephone: (816) 235-6076. Fax: (816) 235-5595. E-mail: Persechinia@umkc.edu.

Funding

This work was supported by National Institutes of Health Grant DK53863 to A.P.

ABBREVIATIONS

CaM, calmodulin; C-lobe and N-lobe, C-terminal and N-terminal lobes in CaM, respectively; B_{IQ}, fluorescent reporter containing an IQ domain sequence derived from neuromodulin; $B_{IQ}G^6A$, $B_{IQ}G^6R$, and $B_{IQ}G^6M$, variants of B_{IQ} with A, R, and M, respectively, substituted for the G at position 6; EB_{IQ}, extended version of B_{IQ} in which the additional neuromodulin sequence, KAHK, has been added on the N-terminal side of the IQ domain insert; $EB_{IQ}A^{-7}E,H^{-6}E$, variant of EB_{IQ} with E substitutions at positions −6 and −7; N_xCCaM (N_xC), mutant CaM with $E^{31}A$ and $E^{67}A$ substitutions in the N-lobe EF hand pair; NC_xCaM (NC_x), mutant CaM with $E^{104}A$ and $E^{140}A$ substitutions in the C-lobe EF hand pair; BAPTA, 1,2-bis(2-aminophenoxy)ethane-*N*,*N*,*N*′,*N*′-tetraacetic acid; dibromo-BAPTA, 1,2-bis(2-amino-5,5′-dibromophenoxy)ethane-*N*,*N*,*N*′,*N*′-tetraacetic acid; ECFP, variant of green fluorescent protein with peak emission at 476 nm; EYFP, variant of green fluorescent protein with peak emission at 527 nm.

REFERENCES

(1) Persechini, A., and Kretsinger, R. H. (1988) The central helix of calmodulin functions as a flexible tether. *J. Biol. Chem. 263*, 12175–12178.

(2) Persechini, A., Moncrief, N. D., and Kretsinger, R. H. (1989) The EF-hand family of calcium-modulated proteins. *Trends Neurosci. 12*, 462–467.

(3) Babu, Y. S., Bugg, C. E., and Cook, W. J. (1988) Structure of calmodulin refined at 2.2 Å resolution. *J. Mol. Biol. 204*, 191–204.

(4) Persechini, A., and Kretsinger, R. H. (1988) Toward a model of the calmodulin-myosin light-chain kinase complex: Implications for calmodulin function. *J. Cardiovasc. Pharmacol. 12*, S1–S12.

(5) Forsén, S., Vogel, H. J., and Drakenberg, T. (1986) Biophysical studies of calmodulin. In *Calcium and Cell Function* (Cheung, W. Y., Ed.) pp 113–157, Academic Press, New York.

(6) Mooseker, M. S., and Cheney, R. E. (1995) Unconventional myosins. *Ann. Rev. Cell Dev. Biol. 11*, 633–675.

(7) Yus-Najera, E., Santana-Castro, I., and Villarroel, A. (2002) The identification and characterization of a noncontinuous calmodulin-binding site in noninactivating voltage-dependent KCNQ potassium channels. *J. Biol. Chem. 277*, 28545–28553.

(8) Jurado, L. A., Chockalingam, P. S., and Jarrett, H. W. (1999) Apocalmodulin. *Physiol. Rev. 79*, 661–682.

(9) Bahler, M., and Rhoads, A. (2002) Calmodulin signaling via the IQ motif. *FEBS Lett. 513*, 107–113.

(10) Black, D. J., and Persechini, A. (2010) Variations at the semiconserved glycine in the IQ domain consensus sequence have a major impact on Ca^{2+}-dependent switching in calmodulin-IQ domain complexes. *Biochemistry 49*, 78–83.

(11) Black, D. J., Selfridge, J. E., and Persechini, A. (2007) The kinetics of Ca^{2+}-dependent switching in a calmodulin-IQ domain complex. *Biochemistry 46*, 13415–13424.

(12) Black, D. J., Leonard, J., and Persechini, A. (2006) Biphasic Ca^{2+}-dependent switching in a calmodulin-IQ domain complex. *Biochemistry 45*, 6987–6995.

(13) Houdusse, A., Gaucher, J. F., Krementsova, E., Mui, S., Trybus, K. M., and Cohen, C. (2006) Crystal structure of apo-calmodulin bound to the first two IQ motifs of myosin V reveals essential recognition features. *Proc. Natl. Acad. Sci. U.S.A. 103*, 19326–19331.

(14) Terrak, M., Rebowski, G., Lu, R. C., Grabarek, Z., and Dominguez, R. (2005) Structure of the light chain-binding domain of myosin V. *Proc. Natl. Acad. Sci. U.S.A. 102*, 12718–12723.

(15) Chagot, B., and Chazin, W. J. (2011) Solution NMR Structure of Apo-Calmodulin in Complex with the IQ Motif of Human Cardiac Sodium Channel NaV1.5. *J. Mol. Biol. 406*, 106–119.

(16) Feldkamp, M. D., Yu, L., and Shea, M. A. (2011) Structural and energetic determinants of apo calmodulin binding to the IQ motif of the Na(V)1.2 voltage-dependent sodium channel. *Structure 19*, 733–747.

(17) Fallon, J. L., Halling, D. B., Hamilton, S. L., and Quiocho, F. A. (2005) Structure of calmodulin bound to the hydrophobic IQ domain of the cardiac Ca(v)1.2 calcium channel. *Structure 13*, 1881–1886.

(18) Van Petegem, F., Chatelain, F. C., and Minor, D. L. (2005) Insights into voltage-gated calcium channel regulation from the structure of the Ca(V)1.2 IQ domain-Ca^{2+}/calmodulin complex. *Nat. Struct. Mol. Biol. 12*, 1108–1115.

(19) Black, D. J., LaMartina, D., and Persechini, A. (2009) The IQ domains in neuromodulin and PEP19 represent two major functional classes. *Biochemistry 48*, 11766–11772.

(20) Persechini, A., and Cronk, B. (1999) The relationship between the free concentrations of Ca^{2+} and Ca^{2+}-calmodulin in intact cells. *J. Biol. Chem. 274*, 6827–6830.

(21) Persechini, A., and Stemmer, P. M. (2002) Calmodulin is a limiting factor in the cell. *Trends Cardiovasc. Med. 12*, 32–37.

(22) Persechini, A. (2002) Monitoring the intracellular free Ca^{2+}-calmodulin concentration with genetically-encoded fluorescent indicator proteins. *Methods Mol. Biol. 173*, 365–382.

(23) Fruen, B. R., Black, D. J., Bloomquist, R. A., Bardy, J. M., Johnson, J. D., Louis, C. F., and Balog, E. M. (2003) Regulation of the RYR1 and RYR2 Ca^{2+} release channel isoforms by Ca^{2+}-insensitive mutants of calmodulin. *Biochemistry 42*, 2740–2747.

(24) Tang, W., Halling, D. B., Black, D. J., Pate, P., Zhang, J. Z., Pedersen, S., Altschuld, R. A., and Hamilton, S. L. (2003) Apocalmodulin and Ca^{2+} calmodulin-binding sites on the Ca(V)1.2 channel. *Biophys. J. 85*, 1538–1547.

(25) Persechini, A., McMillan, K., and Leakey, P. (1994) Activation of myosin light chain kinase and nitric oxide synthase activities by calmodulin fragments. *J. Biol. Chem. 269*, 16148–16154.

(26) Kuznicki, J., Grabarek, H., Brzeska, H., and Drabikowski, W. (1981) Stimulation of enzyme activities by fragments of calmodulin. *FEBS Lett. 130*, 141–145.

(27) Newton, D. L., Oldewurtel, M. D., Krinks, M. H., Shiloach, J., and Klee, C. B. (1984) Agonist and antagonist properties of calmodulin fragments. *J. Biol. Chem. 259*, 4419–4426.

(28) Persechini, A., Yano, K., and Stemmer, P. M. (2000) Ca^{2+} binding and energy coupling in the calmodulin-myosin light chain kinase complex. *J. Biol. Chem. 275*, 4199–4204.

(29) Newman, R. A., Van Scyoc, W. S., Sorensen, B. R., Jaren, O. R., and Shea, M. A. (2008) Interdomain cooperativity of calmodulin bound to melittin preferentially increases calcium affinity of sites I and II. *Proteins 71*, 1792–1812.

(30) Terrak, M., Wu, G. M., Stafford, W. F., Lu, R. C., and Dominguez, R. (2003) Two distinct myosin light chain structures are induced by specific variations within the bound IQ motifs: Functional implications. *EMBO J. 22*, 362–371.

(31) Etter, E. F., Minta, A., Poenie, M., and Fay, F. S. (1996) Near-membrane $[Ca^{2+}]$ transients resolved using the Ca^{2+} indicator FFP18. *Proc. Natl. Acad. Sci. U.S.A. 93*, 5368–5373.

(32) Marsault, R., Murgia, M., Pozzan, T., and Rizzuto, R. (1997) Domains of high Ca^{2+} beneath the plasma membrane of living A7r5 cells. *EMBO J. 16*, 1575–1581.

(33) Davies, E. V., and Hallett, M. B. (1998) High micromolar Ca^{2+} beneath the plasma membrane in stimulated neutrophils. *Biochem. Biophys. Res. Commun. 248*, 679–683.

(34) Klingauf, J., and Neher, E. (1997) Modeling Buffered Ca^{2+} Diffusion Near the Membrane: Implications For Secretion in Neuroendocrine Cells. *Biophys. J. 72*, 674–690.

(35) Simon, S. M., and Llinas, R. R. (1985) Compartmentalization of the submembrane calcium activity during calcium influx and its significance in transmitter release. *Biophys. J. 48*, 485–498.

(36) Llinas, R., and Moreno, H. (1998) Local Ca^{2+} signaling in neurons. *Cell Calcium 24*, 359–366.

(37) Dikici, E., Deo, S. K., and Daunert, S. (2003) Drug detection based on the conformational changes of calmodulin and the fluorescence of its enhanced green fluorescent protein fusion partner. *Anal. Chim. Acta 500*, 237–245.

(38) Yap, K. L., Kim, J., Truong, K., Sherman, M., Yuan, T., and Ikura, M. (2000) Calmodulin target database. *J. Struct. Funct. Genomics 1*, 8–14.

(39) Tadross, M. R., Dick, I. E., and Yue, D. T. (2008) Mechanism of local and global Ca^{2+} sensing by calmodulin in complex with a Ca^{2+} channel. *Cell 133*, 1228–1240.

(40) Dick, I. E., Tadross, M. R., Liang, H., Tay, L. H., Yang, W., and Yue, D. T. (2008) A modular switch for spatial Ca^{2+} selectivity in the calmodulin regulation of CaV channels. *Nature 451*, 830–834.

(41) Gamper, N., and Shapiro, M. S. (2003) Calmodulin mediates Ca^{2+}-dependent modulation of M-type K^+ channels. *J. Gen. Physiol. 122*, 17–31.

(42) Bal, M., Zaika, O., Martin, P., and Shapiro, M. S. (2008) Calmodulin binding to M-type K^+ channels assayed by TIRF/FRET in living cells. *J. Physiol. 586*, 2307–2320.

(43) Wen, H., and Levitan, I. B. (2002) Calmodulin is an auxiliary subunit of KCNQ2/3 potassium channels. *J. Neurosci. 22*, 7991–8001.

(44) Macdougall, D. A., Wachten, S., Ciruela, A., Sinz, A., and Cooper, D. M. F. (2009) Separate elements within a single IQ-like motif in adenylyl cyclase type 8 impart Ca^{2+}/calmodulin binding and autoinhibition. *J. Biol. Chem. 284*, 15573–15588.

(45) Martin, S. R., and Bayley, P. M. (2002) Regulatory implications of a novel mode of interaction of calmodulin with a double IQ-motif target sequence from murine dilute myosin V. *Protein Sci. 11*, 2909–2923.

(46) Schumacher, M. A., Rivard, A. F., Bachinger, H. P., and Adelman, J. P. (2001) Structure of the gating domain of a Ca^{2+}-activated K^+ channel complexed with Ca^{2+}/calmodulin. *Nature 410*, 1120–1124.

(47) Schuster-Bockler, B., Schultz, J., and Rahmann, S. (2004) HMM Logos for visualization of protein families. *BMC Bioinf. 5*, 7.

(48) Finn, R. D., Tate, J., Mistry, J., Coggill, P. C., Sammut, S. J., Hotz, H. R., Ceric, G., Forslund, K., Eddy, S. R., Sonnhammer, E. L., and Bateman, A. (2008) The Pfam protein families database. *Nucleic Acids Res. 36*, D281–D288.